

## Direct Measurement of the Parapositronium Lifetime in $\alpha$ -SiO<sub>2</sub>

Haruo Saito\* and Toshio Hyodo

*Institute of Physics, Graduate School of Arts and Sciences, University of Tokyo, 3-8-1, Komaba,  
Meguru-ku, Tokyo, 153-8902, Japan*

(Received 16 December 2002; published 13 May 2003)

The mean lifetime of delocalized parapositronium in  $\alpha$ -SiO<sub>2</sub> has been determined directly for the first time using a newly developed positron lifetime spectrometer based on BaF<sub>2</sub> scintillators and a fast digital oscilloscope. The lifetime is found to be  $156 \pm 4$  ps, which is much longer than its intrinsic lifetime of 125 ps. This indicates clearly that the primary many-body effect on positronium in  $\alpha$ -SiO<sub>2</sub> is the screening of the Coulomb interaction between the constituent particles by electrons of the medium and that the average distance between the electron and positron in positronium becomes larger than its vacuum value.

DOI: 10.1103/PhysRevLett.90.193401

PACS numbers: 36.10.Dr, 71.35.-y, 78.70.Bj

Positronium (Ps) in  $\alpha$ -SiO<sub>2</sub> has been of continued interest for more than three decades [1–13] ever since Brandt *et al.* identified the delocalized Ps state in the angular correlation of the annihilation radiation (ACAR) spectrum [2]. Ps can exist in either a spin singlet (para) state or a spin triplet (ortho) state. In vacuum, these states have mean lifetimes of 0.125 and 142 ns, respectively [14,15]. The Ps lifetimes in solids differ from their vacuum values due to many-body interactions. One of the many-body effects on Ps in solids is the screening of the Coulomb interaction of the constituent particles by electrons of the medium. This causes the average distance of the electron and positron in Ps to be larger and the contact density of these particles to be smaller. Consequently, an increase is expected in the lifetime of para Ps, which self-annihilates into  $2\gamma$ . For this reason, Ps in solids provides an opportunity for studying the properties of many-body Coulomb interacting systems. Moreover, it also provides complementary information for understanding the physics of excitons and impurities in semiconductors [16] and insulators [17]. The mean lifetime of the Ps in  $\alpha$ -SiO<sub>2</sub>, however, has never been measured directly.

Positron lifetime (PAL) spectra for  $\alpha$ -SiO<sub>2</sub> have been measured by several authors [4,5,8,9]. However, it has been impossible to resolve the para-Ps decay component from those due to ortho Ps, positrons which do not form Ps (free positrons), and positrons trapped in lattice defects. The main reason for this has been the instrumental limitations of the PAL spectrometers used in these works.

Recently, we have developed a new PAL spectrometer [18] using a digital signal processing technique which has a high resolution in addition to high stability and a good signal-to-noise ratio. In the present work, we perform high-statistics measurements of the PAL spectra for  $\alpha$ -SiO<sub>2</sub> with this spectrometer, and determine the mean lifetime of para Ps in  $\alpha$ -SiO<sub>2</sub> directly for the first time.

PAL spectra were measured at room temperature with the newly developed positron lifetime spectrometer [18] consisting of BaF<sub>2</sub> scintillators and a fast digital oscillo-

scope. Samples for these measurements were of size  $7 \times 8 \times 2$  mm<sup>3</sup>, cut from an  $\alpha$ -SiO<sub>2</sub> ingot supplied by Tokyo Denpa Kogyo (Japan). A <sup>22</sup>Na positron source of  $3.7 \times 10^5$  Bq (10  $\mu$ Ci) was deposited directly onto one of the samples and covered with another identical piece. The 1.275 MeV nuclear  $\gamma$  ray, emitted immediately following the positron emission from <sup>22</sup>Na [19], was used to determine the time of the positron injection into the sample, and the 0.511 MeV annihilation  $\gamma$  rays were used to determine the time of the positron annihilation. A schematic diagram of the spectrometer is shown in Fig. 1(a). It differs in a few respects from the setup in Ref. [18]. The present arrangement has four  $\gamma$ -ray detectors, each one consisting of a HAMAMATSU H3378 photomultiplier tube (PMT) and a truncated cone BaF<sub>2</sub> scintillator of size 22–32 mm in diameter and 22 mm in height. Detectors 1 and 2 are “start detectors” that are used to detect the 1.275 MeV  $\gamma$  rays, while detectors A and B are “stop detectors,” used to detect the 0.511 MeV positron annihilation  $\gamma$  rays. The scintillators are shielded by conical lead collimators, as shown in Fig. 1(b), to suppress the Compton scattered  $\gamma$  rays which deteriorate the lifetime spectrum [20]. A Monte Carlo simulation with EGS4 codes [21,22] has shown that the number of events in which a  $\gamma$  ray of 1.275 MeV is Compton scattered in the “start detector” and enters the “stop detector” is reduced by these collimators from  $\sim 1\%$  to less than 0.025%.

Waveforms obtained from the four detectors were stored in a personal computer and, in the off-line analysis, the amplitude, the integrated peak area, and rise time for each waveform were used for the event selection in which abnormal waveforms were automatically rejected. After this step, six independent positron lifetime spectra were obtained simultaneously as follows. When three detectors (1-A-B or 2-A-B) were hit by  $\gamma$  rays in one coincidence event, the event was used for the data of the “double stop” spectra [18]. When only two detectors (1-A, 1-B, 2-A, or 2-B) were hit in coincidence, the event was used for the data of the “single stop” spectra [18].

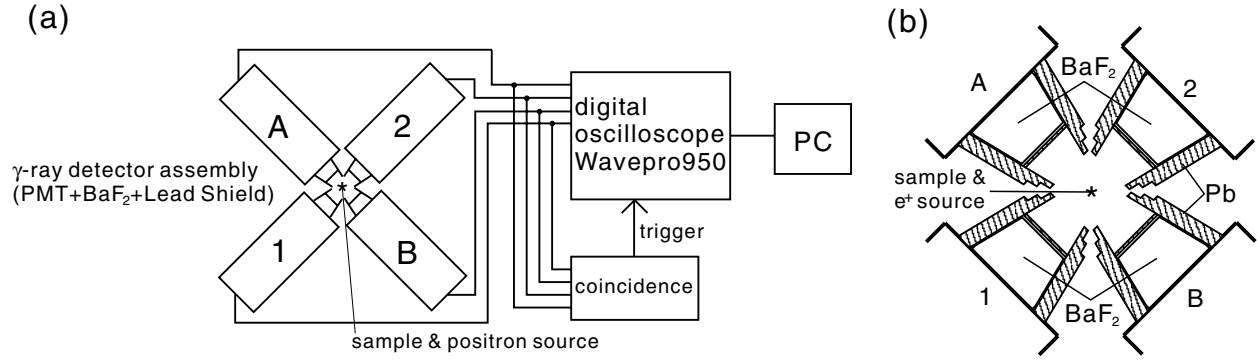


FIG. 1. (a) Schematic diagram of the positron lifetime spectrometer. (b) Magnified view around the positron source and sample.

The momentum distribution of the Ps was measured with a one-dimensional ACAR apparatus [23] in order to obtain the intensity of the self-annihilating para-Ps component. The momentum resolution was set to  $0.453 \times 10^{-3} \text{ mc}$  (0.062 a.u.), and no magnetic field was applied. The sample for the ACAR measurement was cut from the same ingot as that used for the PAL study and all measurements were performed at room temperature.

Figure 2 shows a typical PAL spectrum, obtained from one of the  $\gamma$ -ray detector pairs (1 and A). The small and large dots represent the data before and after background subtraction, respectively. The solid lines showing exponential decay with mean lifetime of 293.5 and 650 ps are guides for the eye. Existence of a short lifetime component is clearly visible in the time range between the peak and channel 150. A long lifetime component of about 650 ps is also visible between channels 350 and 500.

The data are fitted by a sum of three exponentially decaying components. The fitting function,  $f$ , is expressed as

$$f = \left[ \left[ \left[ \Theta(t - t_0) \sum_{i=1}^3 \frac{I_i}{\tau_i} \exp\left(-\frac{t-t_0}{\tau_i}\right) \right] \otimes R_1 \right] \otimes R_2 \right] \otimes R_3, \quad (1)$$

where  $R_1 = \exp[-4 \ln 2 (\frac{t}{\tau_{\text{res}}})^2]$ ,  $R_2 = \Theta(t) \Theta(\tau_{\text{tpc}} - t)$ ,  $R_3 = \exp(\frac{t}{\tau_{1/2}} \ln 2) \Theta(-t)$ ,  $t$  is time,  $t_0$  is the time of the positron injection,  $I_i$  ( $i = 1-3$ ) is the intensity of the  $i$ th component, and  $\tau_i$  is the mean lifetime of the  $i$ th component. Here the sum of three exponentially decaying components is convoluted (as expressed by the symbol  $\otimes$ ) with resolution functions  $R_1$ ,  $R_2$ , and  $R_3$ .  $R_1$  is a Gaussian having a full width at half maximum (FWHM) of  $\tau_{\text{res}}$  to account for the time resolution of the spectrometer.  $R_2$  accounts for the effect of the bin width of the spectrum,  $\tau_{\text{tpc}}$ , and  $R_3$  accounts for the half-life of the  $\gamma$  decay of  $^{22}\text{Na}/^{22}\text{Ne}$ ,  $\tau_{1/2} (= 3.7 \text{ ps})$  [19].  $\Theta(t)$  is the Heaviside step function.

As described above, we obtained six independent PAL spectra at the same time. These spectra were fitted to Eq. (1) simultaneously with independent  $\tau_{\text{res}}$  and  $t_0$  values and with the constraint that the  $\tau_i$  values ( $i = 1-3$ ) were identical for all the spectra. The results are shown in Table I(a). The first component, having the shortest lifetime, results from the decay of the para Ps in  $\alpha$ -SiO<sub>2</sub>. The second component is the mixture of the decays of ortho Ps and free positrons [4]; the third component is due to the decay of positrons in defects. The value of the reduced  $\chi^2$ , 1.04, is close to unity. Considering the very high statistics of the data, this is remarkably good and indicates the reasonableness of the fitted function as well as the stability of the data. The values of the time resolution range from 115 to 160 ps depending on the settings and the characteristics of the PMTs used. The first component is plotted in the inset of Fig. 2. The residues of the fit are plotted in Fig. 3, which indicate very good fitting for all the spectra.

In order to check the reliability of the data, we also performed least squares fits independently to the six spectra. In this analysis, only  $\tau_3$  was fixed (to be 650 ps) while the other parameters were free. The results are shown in Table I(b). It can be seen that the fitting parameters in Table I(b) are statistically consistent with

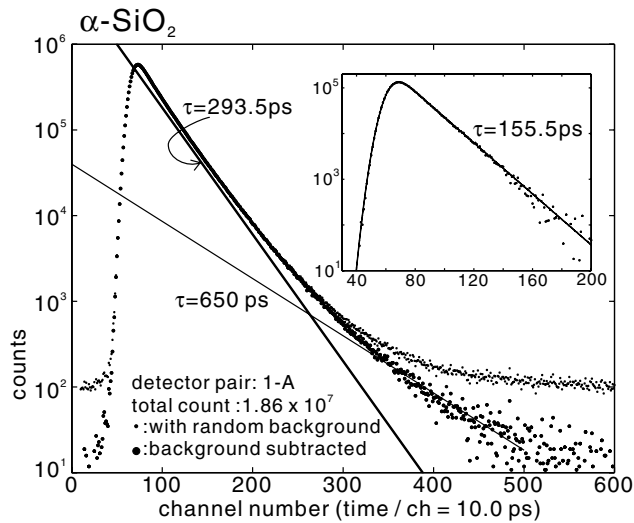


FIG. 2. PAL spectrum measured with one of the  $\gamma$ -ray detector pairs (1 and A). The small and large dots represent the data before and after background subtraction, respectively. The inset shows the data and fitting function after subtracting the background and the second and third components of Eq. (1).

TABLE I. (a) The results of a simultaneous least-squares fit to all data. The values of the time resolution ranges from 115 to 160 ps FWHM. (b) The results of least-square fits for each spectrum. All parameters are free except  $\tau_3$  which is fixed to 650 ps.

Spectrum No.	Detectors	Count number	Time resolution (ps)	$\tau_1$	$I_1$	$\tau_2$	$I_2$	$\tau_3$	$I_3$	Reduced- $\chi^2$
				(ps)	(%)	(ps)	(%)	(ps)	(%)	
(a)										
All		$6.6 \times 10^7$	115–161	$155.5 \pm 2.9$	$16.3 \pm 0.7$	$293.5 \pm 1.7$	$80.3 \pm 1.2$	$650 \pm 15$	$3.4 \pm 0.4$	1.04
(b)										
1	1, A	$1.86 \times 10^7$	133.0	$157.0 \pm 3.1$	$16.5 \pm 0.6$	$293.8 \pm 1.1$	$80.1 \pm 1.1$	650 (fixed)	$3.4 \pm 0.1$	1.04
2	1, B	$1.79 \times 10^7$	150.7	$156.8 \pm 3.4$	$16.1 \pm 0.7$	$293.2 \pm 1.1$	$80.4 \pm 1.2$	650 (fixed)	$3.5 \pm 0.1$	0.93
3	2, A	$1.14 \times 10^7$	144.0	$161.5 \pm 4.1$	$18.1 \pm 0.9$	$295.8 \pm 1.5$	$78.5 \pm 1.6$	650 (fixed)	$3.4 \pm 0.1$	1.11
4	2, B	$1.09 \times 10^7$	160.8	$155.8 \pm 4.5$	$16.4 \pm 0.9$	$293.9 \pm 1.5$	$80.2 \pm 1.5$	650 (fixed)	$3.4 \pm 0.1$	1.01
5	1, A, B	$4.7 \times 10^6$	115.1	$151.0 \pm 5.7$	$16.4 \pm 1.1$	$294.3 \pm 2.2$	$80.5 \pm 2.1$	650 (fixed)	$3.1 \pm 0.1$	1.07
6	2, A, B	$2.9 \times 10^6$	128.0	$144.5 \pm 8.0$	$14.6 \pm 1.4$	$292.2 \pm 2.8$	$82.3 \pm 2.5$	650 (fixed)	$3.2 \pm 0.2$	1.01
Average				$156.4 \pm 1.7$	$16.5 \pm 0.3$	$293.9 \pm 0.6$	$80.1 \pm 0.6$		$3.41 \pm 0.03$	

each other. The averaged values agree well with the results of the simultaneous fit.

The systematic error in the value of  $\tau_1$  is estimated to be  $\pm 2.5$  ps by changing the time span for the fitting, time per channel of the spectrum, energy window, rise time window. By adding the statistical and systematic errors in quadrature, the final results obtained for  $\tau_1$  ( $= \tau_{\text{pPs}}$ ) and  $I_1$  ( $= I_{\text{pPs}}$ ) were

$$\tau_1 = 156 \pm 4 \text{ ps}, \quad I_1 = 16.3 \pm 0.9\%. \quad (2)$$

The ACAR spectrum for  $\alpha$ -SiO<sub>2</sub> is plotted in Fig. 4. The intensity of the narrow component is obtained by subtracting the broad component which is represented by the sum of three Gaussians, and is found to be  $6.9 \pm 0.1\%$ . This component has only contributions from the self-annihilating para Ps, and is smaller than the value of  $I_1$  obtained in the PAL experiment. This is because positrons in the para Ps can also annihilate with electrons in the medium (known as pick-off annihilation), and this process contributes to the broad component in the ACAR spectrum.

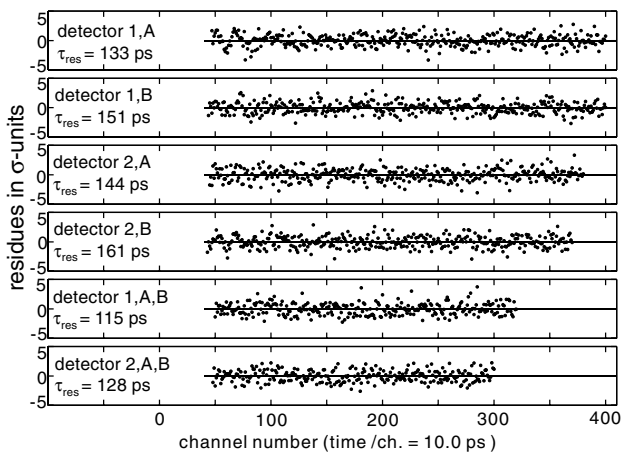


FIG. 3. The residues of the simultaneous least-squares fit to the data using Eq. (1).

The mean lifetimes of para Ps ( $\tau_{\text{pPs}}$ ) and ortho Ps ( $\tau_{\text{oPs}}$ ) in a solid can be written as

$$\begin{aligned} \tau_{\text{pPs}} &= (\kappa\lambda_{2\gamma} + \lambda_{\text{pick-off}})^{-1}, \\ \tau_{\text{oPs}} &= (\kappa\lambda_{3\gamma} + \lambda_{\text{pick-off}})^{-1}, \end{aligned} \quad (3)$$

where  $\lambda_{2\gamma}$  and  $\lambda_{3\gamma}$  are the intrinsic annihilation rates for para Ps [14] and ortho Ps [15] in vacuum, respectively, and  $\lambda_{\text{pick-off}}$  is the pick-off annihilation rate.  $\kappa$  is the electron-positron contact density in Ps relative to that in vacuum and is defined as  $\kappa = \int |\psi(r, r)|^2 dr^3 / \int |\psi_0(r, r)|^2 dr^3$ , where  $\psi(r_e, r_p)$  and  $\psi_0(r_e, r_p)$  are the wave functions of the Ps in the solid and that of the Ps in vacuum, respectively, with  $r_e$  and  $r_p$  being the coordinates of the electron and the positron in Ps. Equations (3) are not self-evident but are justified under a specific condition [24].

Using Eqs. (3),  $\kappa$  and  $\tau_{\text{oPs}}$  can be derived from the results of the present work. Using Eq. (3), the ratio of the self-annihilation of para Ps to its total annihilation is  $R_{\text{self}} = \kappa\lambda_{2\gamma} / (\kappa\lambda_{2\gamma} + \tau_{\text{oPs}}^{-1})$ . This is equal to the ratio of the para-Ps intensity in the ACAR spectrum to that in the PAL spectrum,  $I_N(\text{ACAR})/I_1(\text{PAL})$ . This is because the narrow component in the ACAR spectrum results from only the self-annihilation of para Ps. From this and Eqs. (3), we obtain  $\kappa = 0.34 \pm 0.02$  and  $\tau_{\text{oPs}} = 270 \pm 18$  ps.

In previous work [11], analysis of the magnetic field dependence of Zeeman mixing between ortho Ps and para Ps in  $\alpha$ -SiO<sub>2</sub>, implicitly assuming Eqs. (3), yielded values of  $\kappa = 0.31 \pm 0.02$  and  $\tau_{\text{oPs}} = 273 \pm 9$  ps. These are in agreement with the present result within experimental errors.

The present result of  $\tau_{\text{pPs}} = 156 \pm 4$  ps, which is longer than the para-Ps lifetime in vacuum, shows clearly that Ps atoms are swollen in  $\alpha$ -SiO<sub>2</sub>. The consistency between the present results and that of Zeeman mixing experiments [11] shows the validity of the assumptions implicitly made in the latter work; i.e., the perturbation

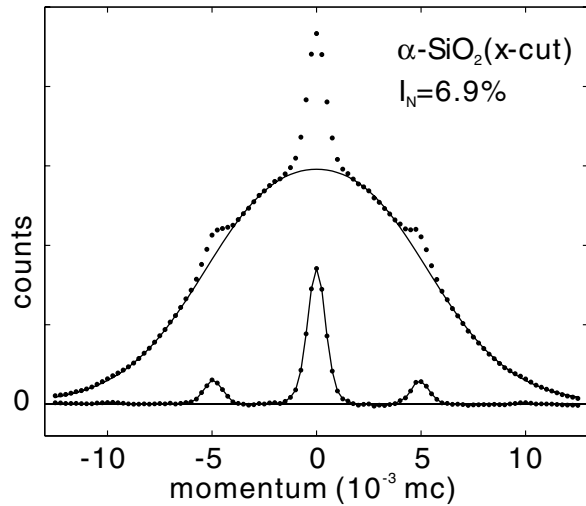


FIG. 4. ACAR spectrum for  $\alpha$ -SiO<sub>2</sub>. No magnetic field is applied.

on delocalized Ps in  $\alpha$ -SiO<sub>2</sub> is described with parameters  $\kappa$  and  $\lambda_{\text{pick-off}}$ , para Ps and ortho Ps are good eigenstates, and the pick-off rate  $\lambda_{\text{pick-off}}$  is practically identical for both para Ps and ortho Ps.

If we regard the Ps in  $\alpha$ -SiO<sub>2</sub> as a hydrogenlike atom bound by the Coulomb potential weakened by the high-frequency dielectric constant  $\epsilon$ , the reduced effective mass of Ps in  $\alpha$ -SiO<sub>2</sub>,  $M_r^*$ , can be estimated using  $M_r^* = (m_e/2)\epsilon/\kappa^{-1/3}$  [1] where  $m_e$  is the free electron mass. Since  $\epsilon$  is equal to the square of refractive index for the visible light, we put  $\epsilon = n^2 \approx 2.4$  and obtain  $M_r^* = 1.7 \times (m_e/2)$ . The total effective mass of Ps in  $\alpha$ -SiO<sub>2</sub>, on the other hand, has been determined to be  $(1.67 \pm 0.15) \times (2m_e)$  [6] or  $(1.54 \pm 0.08) \times (2m_e)$  [12] using the ACAR method. The agreement between these factors is very interesting.

The second component, with a lifetime  $\tau_2$ , in the three component analysis (Table I) is a mixture of the decays of ortho Ps and free positrons. In an attempt to distinguish these two decay components with similar lifetime values, a four component analysis was performed on the PAL spectra. However, this was not successful. Therefore an estimate of the mean lifetime of the free positrons,  $\tau_{\text{free}}$ , was made in the following way. Using  $\tau_{\text{oPs}} = 270$  ps and assuming that the value of  $\tau_2$  obtained in the present work was the weighted average of  $\tau_{\text{oPs}}$  and  $\tau_{\text{free}}$ , we obtain  $\tau_{\text{free}} = (I_2\tau_2 - 3I_1\tau_{\text{oPs}})/(I_2 - 3I_1) = 330$  ps. This estimate is larger than  $\tau_{\text{oPs}}$  and is in contradiction with observations that  $\tau_{\text{oPs}}$  is larger than  $\tau_{\text{free}}$  in many insulating materials [1]. This discrepancy should be investigated in future works.

In conclusion, the mean lifetime of delocalized para Ps in  $\alpha$ -SiO<sub>2</sub> has been determined directly to be  $156 \pm 4$  ps using a newly developed PAL spectrometer. The lifetime

was found to be much longer than its vacuum value. The results are consistent with values from the previous Zeeman mixing study of ortho and para Ps, and provide a clear picture of Ps in  $\alpha$ -SiO<sub>2</sub>.

The authors thank Dr. Y. Nagashima for helpful discussions.

\*Electronic address: saitou@youshi.c.u-tokyo.ac.jp

- [1] A. Dupasquier, in *Positrons in Solids*, edited by P. Hautojarvi (Springer-Verlag, Berlin, 1979), p. 197.
- [2] W. Brandt, G. Coussot, and R. Paulin, *Phys. Rev. Lett.* **23**, 522 (1969).
- [3] A. Greenberger, A. P. Mills, A. Thompson, and S. Berko, *Phys. Lett. A* **32**, 72 (1970).
- [4] C. H. Hodges, B. T. A. McKee, W. Triftshäuser, and A. T. Stewart, *Can. J. Phys.* **50**, 103 (1972).
- [5] A. Bisi, G. Gambarini, and L. Zappa, *Phys. Lett. A* **35**, 193 (1971).
- [6] H. Ikari, *Jpn. J. Appl. Phys.* **19**, L588 (1980).
- [7] P. Sferlazzo, S. Berko, and K. F. Canter, *Phys. Rev. B* **35**, 5315 (1987).
- [8] A. Bisi, G. Consolati, F. Quasso, and L. Zappa, *Nuovo Cimento D* **10**, 1069 (1988).
- [9] S. Dannefaer, T. Friessnegg, D. Kerr, A. Uedono, X. Li, and S. Tanigawa, *Phys. Rev. B* **54**, 15051 (1996).
- [10] Y. Nagashima, Y. Morinaka, T. Kurihara, Y. Nagai, T. Hyodo, T. Shidara, and K. Nakahara, *Phys. Rev. B* **58**, 12676 (1998).
- [11] Y. Nagai, Y. Nagashima, and T. Hyodo, *Phys. Rev. B* **60**, 7677 (1999).
- [12] Y. Nagai, M. Kakimoto, T. Hyodo, K. Fujiwara, H. Ikari, M. Eldrup, and A. T. Stewart, *Phys. Rev. B* **62**, 5531 (2000).
- [13] T. Gessmann, J. Major, A. Seeger, and J. Ehmann, *Philos. Mag. B* **81**, 771 (2001).
- [14] A. H. Al-Ramadhan and D. W. Gidley, *Phys. Rev. Lett.* **72**, 1632 (1994).
- [15] S. Asai, S. Orito, and N. Shinohara, *Phys. Lett. B* **357**, 475 (1995).
- [16] E. F. Schubert, *Doping in III-V Semiconductors* (Cambridge University Press, Cambridge, U.K., 1993).
- [17] Y. Toyozawa, *J. Lumin.* **24/25**, 23 (1981).
- [18] H. Saito, Y. Nagashima, T. Kurihara, and T. Hyodo, *Nucl. Instrum. Methods Phys. Res., Sect. A* **487**, 612 (2002).
- [19] *Table of Isotopes*, edited by C. M. Lederer and V. S. Shirley (John Wiley & Sons, Inc., New York, 1978), 7th ed.
- [20] T. B. Chang, D. Yin, C. Cao, and S. Wang, *Nucl. Instrum. Methods Phys. Res., Sect. A* **256**, 398 (1987).
- [21] W. R. Nelson, H. Hirayama, and D. W. O. Rogers, Report No. SLAC-265, 1985.
- [22] Y. Namito and H. Hirayama, *Nucl. Instrum. Methods Phys. Res., Sect. A* **423**, 238 (1999).
- [23] J. Kasai, T. Hyodo, and K. Fujiwara, *J. Phys. Soc. Jpn.* **57**, 329 (1988).
- [24] A. Dupasquier, P. DeNatale, and A. Rolando, *Phys. Rev. B* **43**, 10036 (1991).